Supporting Information

Kuraoka et al. 10.1073/pnas.1102571108

SI Materials and Methods

Mice. Female C57BL/6 (B6, CD45.2), B6.SJL-*Ptprc*^{a} *Pepc*^{b}/BoyJ (CD45.1), (B6.SJL × B6)F_1 (CD45.1/CD45.2) mice, and congenic B6(B6CB)-*Aicda*^{tm1Hon} animals deficient for AID (*Aicda*$^{-/-}$, CD45.2) (1), *Aicda*$^{-/-}$*Cd154*$^{-/-}$ [*Aicda*$^{-/-}$ × *Cd154*$^{-/-}$ (2)], 3H9 heavy chain knock-in (3), 3H9*Aicda*$^{-/-}$ (3H9 × *Aicda*$^{-/-}$), *C4*$^{-/-}$, and *Rag1*$^{-/-}$ mice (all B6 background) were bred and maintained under specific pathogen-free conditions at the Duke University Animal Care Facility. Mice used in experiments were 7 to 12 wk of age except for *C4*$^{-/-}$ mice (sera were collected at 5–6 mo). All experiments involving animals were approved by the Duke University Institutional Animal Care and Use Committee.

Flow Cytometry and Definition of Hematopoietic Populations. Frequencies of CD45^{+} donor and host cells in BM chimeric animals were determined by flow cytometry, and specific hematopoietic compartments were identified as follows (Fig. S2). Progenitors: LSK cells were determined as B220^{-}CD4^{-}CD8^{-}CD11b^{-}Gr-1^{-}TER119^{-} (Lin^{-}) Sca-1^{+}Kit^{+} cells in the BM (4). Myeloid-lineage cells: CMP (Lin^{-}Sca-1^{-}Kit^{+}CD34^{+}FcγR^{-}), granulocyte macrophage progenitor (Lin^{-}Sca-1^{-}Kit^{+}CD34^{+}FcγR^{+}), myelocyte (Ly6G$^{low/-}$7/4$^{int/-}$) and mature neutrophils (Ly6G^{high}7/4^{int}) in the BM, and myeloid (B220^{-}CD3^{-}CD11b^{+}) cells in spleen. B-lineage cells: pro-/pre-B (B220^{low}CD93^{+}IgM^{-}IgD^{-}), pro-B (B220^{low}CD93^{+}IgM^{-}IgD^{-}CD43^{+}), large pre-B (B220^{low}CD93^{+}IgM^{-}IgD^{-}CD43^{-}FSC^{high}), small pre-B (B220^{low}CD93^{+}IgM^{-}IgD^{-}CD43^{-}FSC^{low}), im/T1 B (B220^{low}CD93^{+}IgM^{+}IgD^{-}), immature B (B220^{low}CD93^{+}IgM^{low}IgD^{-}CD23^{-}), T1 B (B220^{low}CD93^{+}IgM^{high}IgD$^{+/-}$CD23^{-}), and mature B (B220^{hi}CD93^{-}IgM^{int}IgD^{hi}) cells in the BM, and T1/T2 B (B220^{low}CD93^{+}IgM^{high}IgD$^{+/-}$), T1 B (B220^{low}CD93^{+}IgM^{high}IgD$^{+/-}$CD23^{-}), T2 B (B220^{low}CD93^{+}IgM^{high}IgD$^{+/-}$CD23^{+}), mature follicular B (B220^{high}CD93^{-}IgM^{int}IgD^{high} or B220^{high}CD93^{-}IgM^{int}IgD^{high}CD21^{low}CD23^{high}) and marginal-zone B (B220^{high}CD93^{-}IgM^{high}IgD^{low} or B220^{high}CD93^{-}IgM^{high}IgD^{low}CD21^{high}CD23^{low}) cells in blood and spleen (5, 6), and GC B (GL-7^{+}B220^{high}Fas^{+}IgD^{-}) cells in PPs. T-lineage cells: B220^{-}CD11b^{-}Gr-1^{-}CD11c^{-}Ter119^{-} fraction of thymocytes were further divided by expression pattern of CD4 and CD8 into double negative (CD4^{-}CD8^{-}), double positive (DP; CD4^{+}CD8^{+}), CD4 single positive (CD4 SP; CD4^{+}CD8^{-}), and CD8 single positive (CD8 SP; CD4^{-}CD8^{+}) compartments. Cells that take up propidium iodide were excluded from our analyses. Labeled cells were analyzed/sorted in a FACS Canto (BD Bioscience) or FACS Vantage with DIVA option (BD Bioscience). Flow cytometric data were analyzed with FlowJo software (Treestar).

Quantitative RT-PCR and Quantification of AID Expression. Expression of AID mRNA was determined by a quantitative RT-PCR (7) referenced to a synthetic standard. Briefly, total RNA was extracted from sorted hematopoietic cell populations (2.0×10^4 cells) and cDNA was prepared by standard methods (7). One-twentieth volume of cDNA samples or various concentrations of AID cDNA templates (as detailed later) were amplified in a primary PCR using Ramp-Taq DNA polymerase (Denville Scientific) with AID118 and AID119 primers (1). Primary PCR condition was as follows: initial incubation of 95 °C for 7 min followed by 15 cycles of amplification steps (95 °C for 30 s, 60 °C for 20 s, and 72 °C for 45 s). Then, primary PCR products were subjected to quantitative PCR using SYBR Green core reagents and AIDF2/AIDR2 primers (7).

AID cDNA templates were made as follows. Murine AID transcript (708 bp, 5′-UTR plus entire coding region plus restriction enzyme sites for cloning into vector) was amplified from cDNA of 103/BCL2 cell line (8) using a specific primer pair (5′-AAACTCGAGGTCACACAACAGCACTGAAGCA-3′ and 5′-TTTTCTAGATCAAAATCCCAACATACGAAATG-3′) and cloned into pBS II SK (+) vector (Invitrogen). To distinguish AID cDNA templates from endogenous AID cDNA, 20 bp oligo DNA that contain *HindIII* recognition sequence at the *XmaI* restriction site of the murine AID transcript was inserted into the templates. Then the AID cDNA templates were digested from the vector and concentration of the AID cDNA templates was determined by spectrophotometer. Serially diluted AID cDNA templates were introduced into standard quantity of cDNA from *Aicda*$^{-/-}$ splenocytes. Samples were then subjected to the nested PCR described earlier. A highly significant (R^2 = 0.99) linear relationship between template number and C_T values was obtained (Fig. S1*A*) for samples that generated amplicand; this curve was used subsequently to quantify the numbers of endogenous AID cDNA copies present in purified samples of hematopoietic cells. Detection limit of the assay was determined by limiting dilution assay of low numbers of AID cDNA templates (Fig. S1*B*). The frequency of negative PCR reactions (71%) in samples containing four standard template copies indicates that 10 replicate PCR amplifications will reliably detect (95%) no more than four copies of endogenous AID cDNA in samples of 10^3 cells.

Competitive Hematopoietic Reconstitution. (B6.SJL × B6)F_1 mice (CD45.1^{+}/CD45.2^{+}) were sublethally irradiated (6.5 Gy) and reconstituted with equal numbers of nonadherent BM cells (5×10^6 each) from B6.SJL (CD45.1^{+}) and B6 (CD45.2^{+}) or *Aicda*$^{-/-}$ (CD45.2^{+}) mice. Six weeks after reconstitution, chimeric mice were killed and frequencies of CD45.1^{+}CD45.2^{-}, CD45.1^{-}CD45.2^{+} (donor), and CD45.1^{+}CD45.2^{+} (host) cells in the myeloid and lymphoid compartments of BM, thymus, spleen, and PP were determined by standard flow cytometric criteria (Fig. S2). At this time, at least 95% of CD45^{+} cells in myeloid-, B-lymphoid, and thymic T-lineage compartments were derived from donor progenitors (CD45.1^{+}CD45.2^{-} or CD45.1^{-}CD45.2^{+}). In the spleen, 10% to 20% of CD4^{+} and CD8^{+} T cells were of host origin (CD45.1^{+}CD45.2^{+}).

ELISA for Detection of Anti-DNA Antibody and Self-Reactive Antibody. Anti- dsDNA and self-reactive Igκ antibody in sera from B6, *Aicda*$^{-/-}$, *C4*$^{-/-}$, and *Rag1*$^{-/-}$ mice was measured by ELISA. Detection of anti-dsDNA antibody was described (9) except for the use of mouse dsDNA antibody HYB331-01 (IgG2a/κ; Abcam) and HRP-labeled goat anti-mouse Igκ antibody (Southern Biotech) as standard and detection antibodies, respectively. The levels of self-reactive Igκ or IgM antibody in sera from B6, *Aicda*$^{-/-}$, and *Aicda*$^{-/-}$*Cd154*$^{-/-}$ mice were determined by the reactivity to NIH 3T3 cell line. For the determination of self-reactive IgM, serum IgM levels in each sample were determined by standard sandwich ELISA before the assay, and then sera were diluted to 400 μg IgM/mL. Briefly, NIH 3T3 cells were cultured overnight in 96-well plates and then fixed in situ well with acetone:methanol (1:1 ratio). After washing with PBS solution containing 0.5% BSA/0.1% Tween 20, wells were blocked with 1% BSA in PBS solution. Subsequently, serially diluted sera were added to each well and incubated for 2 h at room temperature. After washing, HRP-labeled goat anti-mouse Igκ or anti-mouse IgM antibody were added for 1 h at room temperature. After extensive washing, bound HRP activity was visualized

using a TMB peroxidase kit (Bio-Rad Laboratories), and optical densities were determined at 450 nm.

ELISA for Detection of Serum BAFF Concentration. Serum BAFF levels in B6 and *Aicda*$^{-/-}$ mice were compared by standard sandwich ELISA (Fig. S4*A*). Briefly, 96-well ELISA plates were coated with anti-BAFF antibody (clone 121808; R&D Systems) in carbonate buffer overnight. After blocking plates with PBS solution containing 1% FCS, serially diluted sera or recombinant mouse BAFF (R&D Systems) were added to each well and plates were incubated at 37 °C for 1 h. After washing, recombinant mouse BAFF-R/Fc (R&D Systems) was added and incubated at 37 °C for 1 h. After washing, HRP-labeled rabbit anti-human IgG was added for 30 min at room temperature. After extensive washing, bound HRP activity was visualized by using a TMB peroxidase kit (Bio-Rad Laboratories), and optical densities were determined at 450 nm.

Immunofluorescence. The presence of anti-DNA/nuclear Igκ antibody and self-reactive Igκ antibody in serially diluted sera from 8- to 10-wk B6, *Aicda*$^{-/-}$, 3H9, or 3H9.*Aicda*$^{-/-}$ mice were screened on *C. luciliae* and on NIH 3T3 cells as described (10). Pooled sera from age-matched *Rag1*$^{-/-}$ mice and 5- to 6-mo *C4*$^{-/-}$ mice were used as negative and positive controls, respectively. Representative images were photographed (exposure times of 0.3 s for anti-DNA/nuclear Igκ antibody and 1.5 s for self-reactive Igκ antibody) by using an Axiovert 200M microscope with AxioCam MRm and AxioVision AC 4.5 software (Zeiss).

Detection of CD4$^+$Foxp3$^+$ Regulatory T Cells. Frequencies and numbers of splenic regulatory T cells were compared in B6 and *Aicda*$^{-/-}$ mice (Fig. S4 *B* and *C*). Splenocytes from B6 and *Aicda*$^{-/-}$ mice were labeled with antibodies against mouse CD4 (FITC) and Foxp3 (PE) by using a Mouse Regulatory T Cell Staining Kit (eBioscience) following the instructions of the manufacturer.

Amplification of 3H9 VDJ Rearrangements. The retention of 3H9 VDJ rearrangements in genomic DNA from B-cell subsets were determined by quantitative PCR. Briefly, genomic DNA was isolated by phenol-chloroform extraction from sorted BM immature/T1 B cells, splenic mature follicular B cells, and thymocytes from 3H9 and 3H9.*Aicda*$^{-/-}$ mice and was subjected to quantitative PCR with primer pairs 3H9LD_F/3H9CDR3_R (11) and CD14L/CD14R (12). The relative expression levels of 3H9 VDJ rearrangements to CD14 gene were calculated by the comparative threshold cycle method (7).

The mutation frequency in 3H9 VDJ rearrangements amplified from genomic DNA of 3H9 and 3H9.*Aicda*$^{-/-}$ BM immature/T1 B cells, and 3H9 PP GC B cells was compared by sequencing. Briefly, 3H9 and *Cd14* alleles in 5×10^3 sorted cells were amplified by a nested PCR by *Pfu* turbo polymerase (Stratagene) with primer pairs described earlier (11). After theinitial 30 cycles of amplification, a second round of 30 cycles was performed with the internal primers 3H9LD_F in: 5′-tgt cag gaa ctg cag gta agg a-3′ and 3H9CDR3_R in: 5′-aac ata gga ata ttt act cct cgc tct-3′. Amplified VDJ products were cloned using Zero Blunt TOPO PCR cloning kit (Invitrogen) and were sequenced in an Applied Biosystems automated DNA sequencer and analyzed with comparison with the original 3H9 VDJ sequence (13).

Cell Culture. The susceptibility of immature/T1 B cells from *Aicda*$^{+/+}$ and *Aicda*$^{-/-}$ BM to anti-IgM antibody induced apoptosis was compared in cell culture (14). BM cells (1×10^6) from B6 and *Aicda*$^{-/-}$ mice were cultured in triplicate in media containing various concentrations (0, 0.1, 1, 3, and 10 μg/mL) of F(ab)′$_2$ fragment of anti-IgM (anti-μ) antibody (Jackson Immunoresearch). After 24 h, live cells were counted and labeled with fluorescent tagged monoclonal antibodies, and frequencies/numbers of immature/T1 B cells (B220$^+$CD93$^+$IgD$^{+/-}$Igκ$^+$ or -Igλ$^+$; Fig. S7) were determined by flow cytometry.

Statistical Analyses of Data. Statistical significance (at $P \leq 0.05$, $P \leq 0.01$, or $P \leq 0.001$) in paired data was determined by two-tailed Student *t* test.

1. Muramatsu M, et al. (2000) Class switch recombination and hypermutation require activation-induced cytidine deaminase (AID), a potential RNA editing enzyme. *Cell* 102:553–563.
2. Renshaw BR, et al. (1994) Humoral immune responses in CD40 ligand-deficient mice. *J Exp Med* 180:1889–1900.
3. Chen C, Nagy Z, Prak EL, Weigert M (1995) Immunoglobulin heavy chain gene replacement: a mechanism of receptor editing. *Immunity* 3:747–755.
4. Ikuta K, Weissman IL (1992) Evidence that hematopoietic stem cells express mouse c-kit but do not depend on steel factor for their generation. *Proc Natl Acad Sci USA* 89: 1502–1506.
5. Li YS, Wasserman R, Hayakawa K, Hardy RR (1996) Identification of the earliest B lineage stage in mouse bone marrow. *Immunity* 5:527–535.
6. Allman D, et al. (2001) Resolution of three nonproliferative immature splenic B cell subsets reveals multiple selection points during peripheral B cell maturation. *J Immunol* 167:6834–6840.
7. Ueda Y, Liao D, Yang K, Patel A, Kelsoe G (2007) T-independent activation-induced cytidine deaminase expression, class-switch recombination, and antibody production by immature/transitional 1 B cells. *J Immunol* 178:3593–3601.
8. Chen YY, Wang LC, Huang MS, Rosenberg N (1994) An active v-abl protein tyrosine kinase blocks immunoglobulin light-chain gene rearrangement. *Genes Dev* 8: 688–697.
9. Chen Z, Koralov SB, Kelsoe G (2000) Complement C4 inhibits systemic autoimmunity through a mechanism independent of complement receptors CR1 and CR2. *J Exp Med* 192:1339–1352.
10. Holl TM, Haynes BF, Kelsoe G (2010) Stromal cell independent B cell development in vitro: Generation and recovery of autoreactive clones. *J Immunol Methods* 354:53–67.
11. Erikson J, et al. (1991) Expression of anti-DNA immunoglobulin transgenes in non-autoimmune mice. *Nature* 349:331–334.
12. Constantinescu A, Schlissel MS (1997) Changes in locus-specific V(D)J recombinase activity induced by immunoglobulin gene products during B cell development. *J Exp Med* 185:609–620.
13. Shlomchik MJ, Aucoin AH, Pisetsky DS, Weigert MG (1987) Structure and function of anti-DNA autoantibodies derived from a single autoimmune mouse. *Proc Natl Acad Sci USA* 84:9150–9154.
14. Hertz M, Nemazee D (1997) BCR ligation induces receptor editing in IgM+IgD- bone marrow B cells in vitro. *Immunity* 6:429–436.

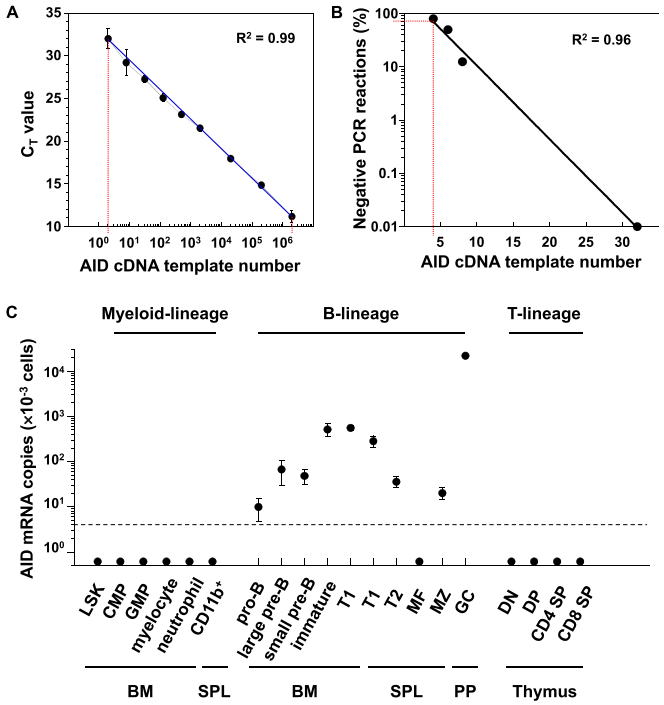

Fig. S1. AID mRNA expression in developing B cells but not in other hematopoietic lineages. AID mRNA copies were quantified by quantitative RT-PCR using an artificial AID cDNA template. (*A*) Threshold cycle (C_T) values are highly correlated to AID cDNA template numbers over a wide range (2–2 × 10^6 copies) of template concentrations. (*B*) Limiting dilution assay of low numbers of AID cDNA templates indicates that 10 replicate PCR amplifications will reliably detect (95%) no more than four copies of endogenous AID cDNA in samples of 10^3 cells. (*C*) AID mRNA was undetectable (<4 copies/10^3 cells) in hematopoietic progenitors, and in cells committed to the T- or myeloid lineages. AID expression was detected in pro-B cells (10 ± 5 copies/10^3 cells) and increased in large and small pre-B cells (68 ± 38 copies/10^3 cells and 49 ± 17 copies/10^3 cells, respectively). AID mRNA transcripts were highest in immature and T1 B cells from BM (520 ± 160 copies/10^3 cells and 560 ± 79 copies/10^3 cells, respectively), were lower in splenic T1 B cells (290 ± 80 copies/10^3 cells), and decreased precipitously in splenic T2 (36 ± 9.0 copies/10^3 cells) and mature B cells (<4.0 copies/10^3 cells). GC B cells expressed the highest levels of AID mRNA (22,000 ± 1,600 copies/10^3 cells). The detection limit of this method, no more than four mRNA copies/10^3 cells (Fig. S1*B*) is indicated by a dashed horizontal line.

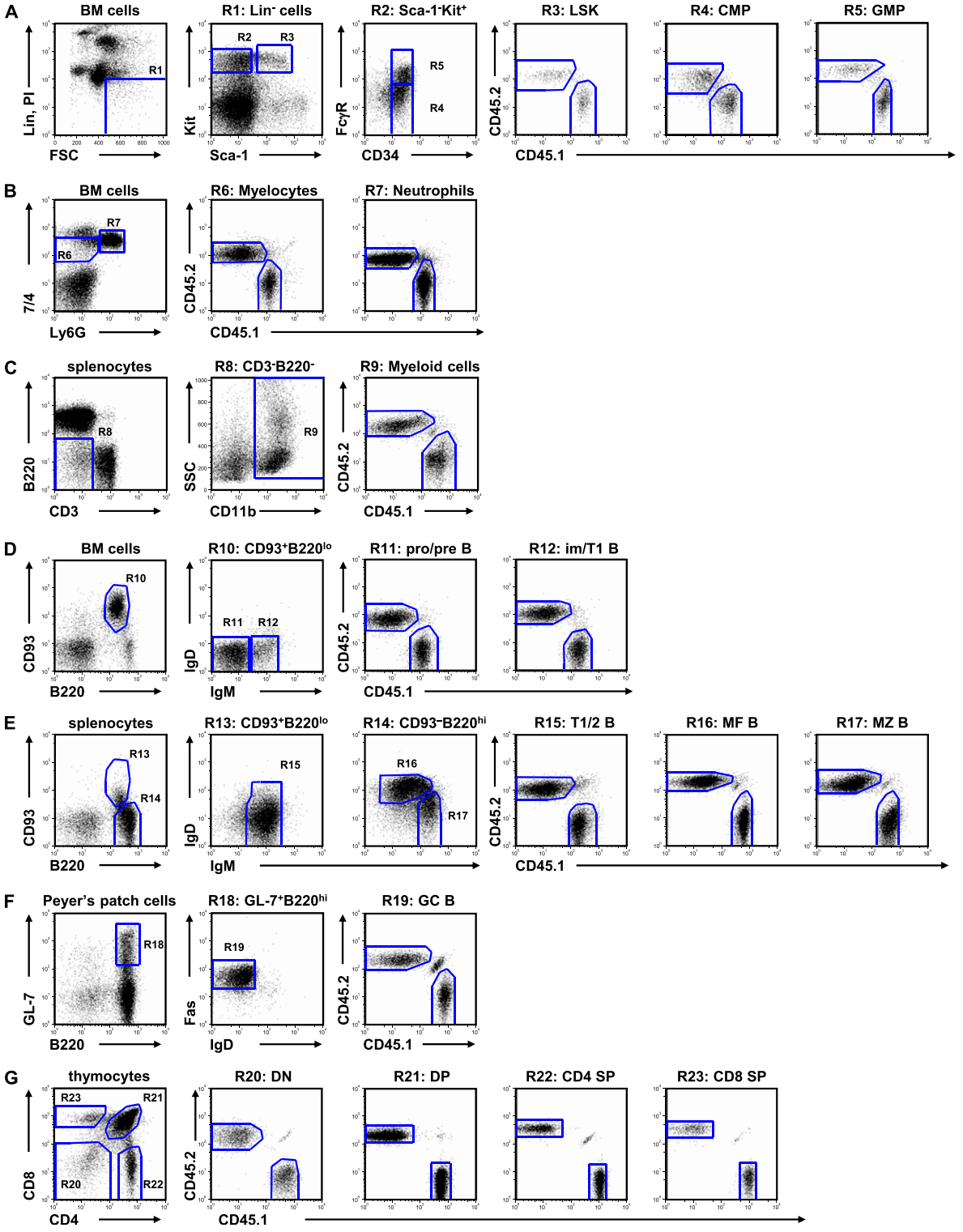

Fig. S2. Identification of donor-derived CD45.1$^+$CD45.2$^-$ cells and CD45.1$^-$CD45.2$^+$ cells in progenitors, myeloid-, B-, and T-lineage cell compartments of reconstituted mice. (*A*) Lin$^-$ (CD4$^-$CD8$^-$CD11b$^-$CD11c$^-$B220$^-$Gr-1$^-$Ter119$^-$) BM cells (R1) were divided by Sca-1, Kit, CD34, and FcγR expression into LSK (R3), CMP (R4), and granulocyte macrophage progenitor (R5) compartments. (*B*) BM cells were divided by Ly-6G and 7/4 expression into myelocyte (R6) and neutrophil (R7) compartments. (*C*) Splenocytes that express CD3 or B220 were excluded (R8), and CD11b$^+$ cells (R9) in remaining cells were determined as a splenic myeloid-lineage cell compartment. (*D*) Developing B-cell compartment (R10) in the BM was identified by B220 and CD93 expression, and was further divided by IgM and IgD expression into pro-/pre- (R11) and immature/T1 (R12) B-cell compartments. (*E*) Splenic developing (R13) and mature (R14) B-cell compartments were identified by B220 and CD93 expression. T1/T2 B-cell compartment (R15) was identified as IgM$^+$IgD$^{+/-}$ fraction of the developing B-cell compartment. Mature B-cell compartment was further divided by IgM/IgD expression into mature follicular (R16) and marginal zone (R17) B-cell compartments. (*F*) PP GC B-cell compartment (R19) was identified as IgD$^-$Fas$^+$ fraction of GL-7$^+$B220^{high} (R18) PP cells. (*G*) B220$^-$CD11b$^-$Gr-1$^-$CD11c$^-$Ter119$^-$ fraction of thymocytes were further divided by expression pattern of CD4 and CD8 into double negative (R20), double positive (DP; R21), CD4 single positive (CD4 SP; R22), and CD8 single positive (CD8 SP; R23) compartments. CD45.1/-0.2 expressions in each compartment are shown.

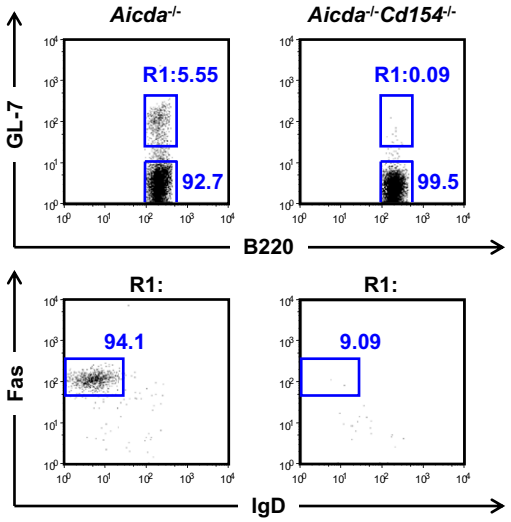

Fig. S3. Constitutive splenic GC formations in *Aicda*$^{-/-}$ mice are CD154-dependent. Splenocytes from naive *Aicda*$^{-/-}$ and *Aicda*$^{-/-}$*Cd154*$^{-/-}$ mice were labeled with fluorescent tagged mAb against mouse B220, CD93, GL-7, Fas, and IgD to delineate GC B cells. Representative flow diagrams are shown. Upper panels are pregated on B220^{hi}CD93^{-} mature B-cell compartment. Numbers near the boxes indicate the frequencies of cells within those boxes.

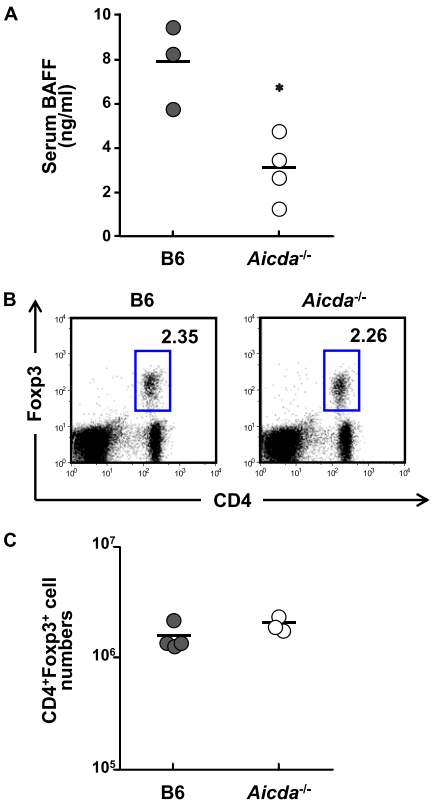

Fig. S4. Reduced serum BAFF and normal splenic regulatory T cells in *Aicda*$^{-/-}$ mice. Serum BAFF levels and frequencies/numbers of splenic regulatory T cells were compared in B6 and *Aicda*$^{-/-}$ mice. (*A*) Serum BAFF concentration was determined by ELISA. (*B*) Representative flow diagrams for CD4 and Foxp3 expression by splenocytes are shown (frequencies of CD4^{+}Foxp3^{+} regulatory T cells in splenocytes are indicated as numbers near the boxes). (*C*) Splenic CD4^{+}Foxp3^{+} regulatory T cell numbers are shown. In *A* and *C*, each symbol represents data from an individual mouse.

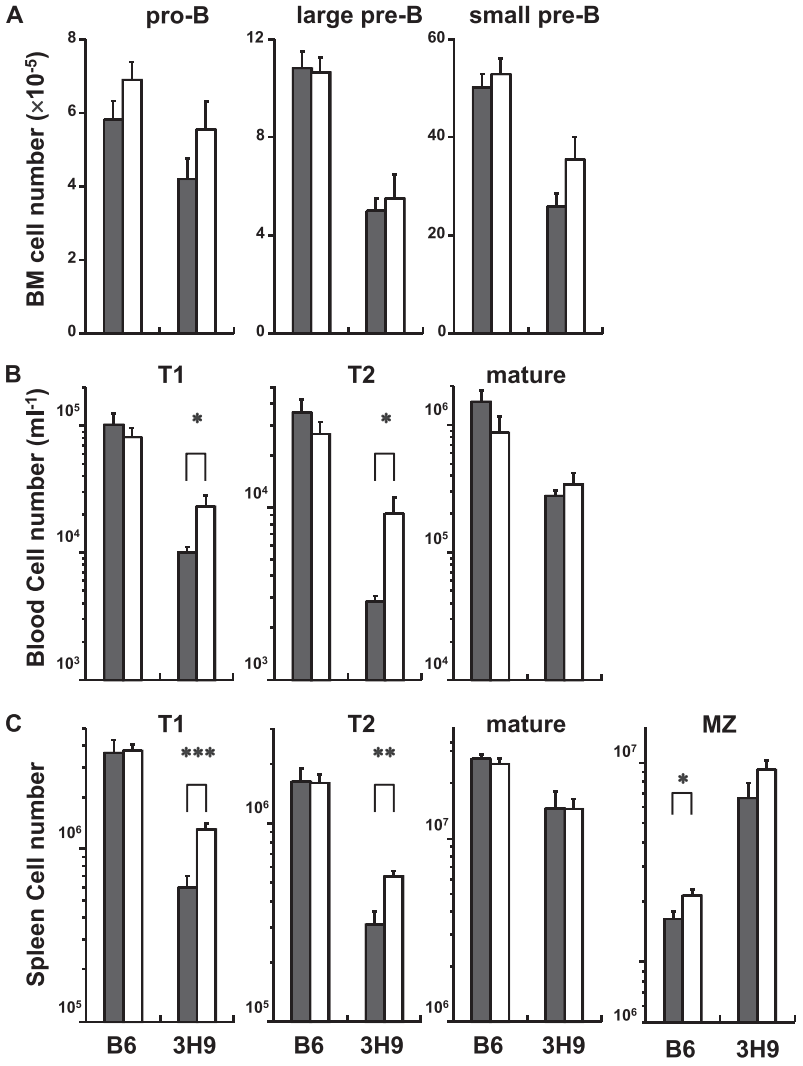

Fig. S5. Absolute cell number of B-cell compartments among B6, *Aicda*$^{-/-}$, 3H9, and 3H9.*Aicda*$^{-/-}$ mice. Numbers of pro-B and small and large pre-B cells in the BM (*A*); and T1, T2, mature, and/or marginal zone (MZ) B cells in blood (*B*) and spleen (*C*) from B6 (*Aicda*$^{+/+}$, filled bars; *Aicda*$^{-/-}$ open bars) and 3H9 (*Aicda*$^{+/+}$, filled bars; *Aicda*$^{-/-}$ open bars) mice are shown. Histograms represent mean values ± SEM (n = 7–10). All statistically significant differences (two-tailed Student t test) are indicated (*P < 0.05, **P < 0.01, ***P < 0.001).

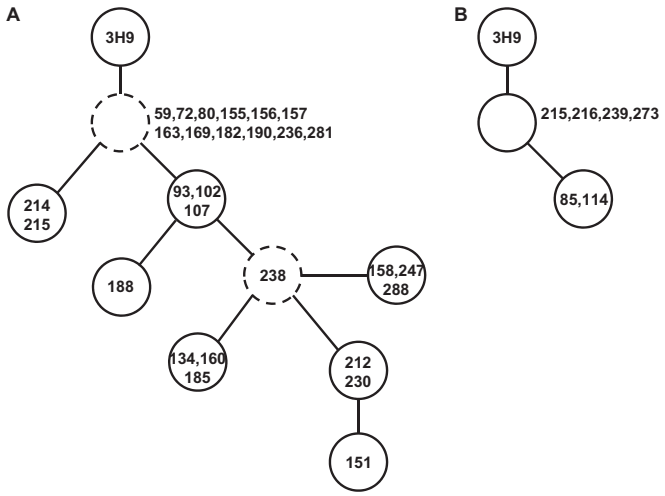

Fig. S6. Genealogical relationship of 3H9 VDJ DNA sequences derived from PP GC B cells. Point mutations were determined by comparison with original 3H9 VDJ sequence. Numbers in circles represent nucleotide positions that are additionally mutated from 3H9 VDJ sequences of adjacent node. Hypothetical intermediates are shown in broken lines. Examples are shown in *A* and *B*.

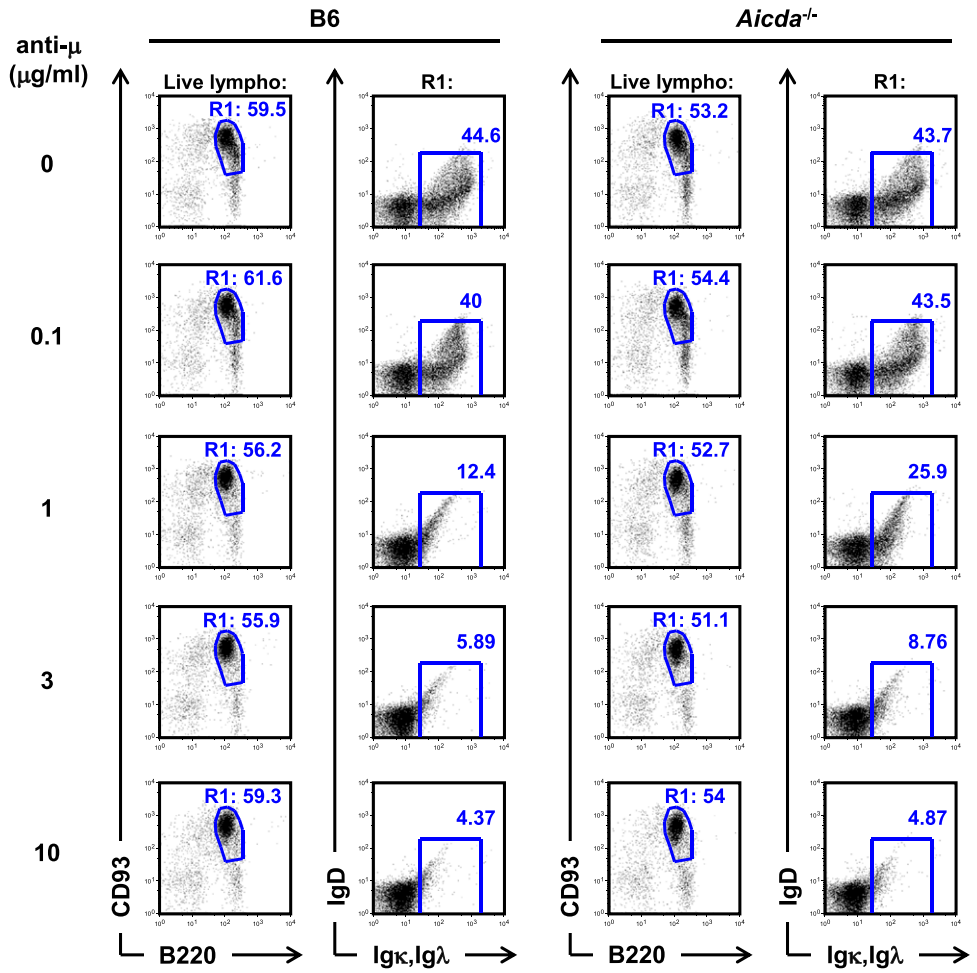

Fig. S7. Immature/T1 B cells from BM of *Aicda*$^{-/-}$ mice are more resistant to anti-IgM–induced apoptosis. Frequencies of surface Ig^{+}(κ^{+} or λ^{+})IgD$^{+/-}$CD93^{+}B220^{lo} immature/T1 B-cell compartments in BM cells from B6 and *Aicda*$^{-/-}$ mice were compared after stimulation with 0, 0.1, 1, 3, and 10 μg/mL of anti-IgM Ab for 24 h. Representative flow diagrams are shown. Numbers in flow diagrams indicate the frequencies of cells in boxes.

Table S1. SHM in im/T1 B cells from 3H9 mice

Finding	*Aicda*$^{+/+}$ im/T1 B	*Aicda*$^{-/-}$ im/T1 B	*Aicda*$^{+/+}$ GC B
No. of 3H9 VDJ rearrangements	45	51	20
Base pairs sequenced	1.3×10^4	1.5×10^4	0.6×10^4
No. of unique mutations	12	0	47
No. of mutated rearrangements (% total)	9 (20%)	0 (0%)	13 (65%)
Mutation frequency*	9.2×10^{-4}	$<0.7 \times 10^{-4}$	81×10^{-4}
RGYW/WRCY† Δhotspot/Δtotal (%)	3/12 (25%)	NA	8/47 (17%)
Mutations at C/G, % total	67	NA	49
ΔR:ΔS‡	8:4	NA	39:8

3H9 V_HDJ_H rearrangements were amplified from genomic DNA of BM im/T1 B cells and PP GC B cells by PCR, cloned into bacteria, and sequenced. NA, not applicable.

*The mutation frequency is calculated by numbers of unique mutations/base pairs sequenced.

†Numbers of mutation in RGYW/WRCY motifs (Δhotspot), total numbers of unique mutations (Δtotal), and percentages of Δhotspot in Δtotal are shown.

‡Numbers of replacement mutations (ΔR) and silent mutations (ΔS) are shown.